

Title	Weldability of Molybdenum and Its Alloy Sheet (Report I)(Materials, Metallurgy, Weldability)
Author(s)	Matsuda, Fukuhisa; Ushio, Masao; Nakata, Kazuhiro; Edo, Yoshiaki
Citation	Transactions of JWRI. 8(2) P.217-P.229
Issue Date	1979-12
Text Version	publisher
URL	http://hdl.handle.net/11094/3996
DOI	
rights	本文データはCiNiiから複製したものである
Note	

Osaka University Knowledge Archive : OUKA

<https://ir.library.osaka-u.ac.jp/>

Osaka University

Weldability of Molybdenum and Its Alloy Sheet (Report I)[†]

Fukuhisa MATSUDA*, Masao USHIO**, Kazuhiro NAKATA*** and Yoshiaki EDO****

Abstract

Basic weldability of electron-beam melted pure molybdenum has been examined in electron-beam welding in high vacuum and GTA welding in pure and air mixed argon atmospheres by paying attention to weld defects such as hot cracking and porosity in weld metal and also mechanical properties of welded joint in comparison with conventional TZM alloys. The main conclusions obtained were as follows; (1) The weld metals of electron-beam melted pure molybdenum with electron-beam and GTA weldings in pure and air mixed argon atmosphere up to about 1% were almost porosity free. However, large amount of oxygen content of 200 ppm in powder-metallurgy TZM alloy made very porous weld bead in electron-beam welding in high vacuum. Therefore, oxygen content in base metal should be lowered to the minimum, that is, less than 10 ppm, especially in electron-beam welding in high vacuum. (2) Hot cracking occurred in the weld metal of GTA welding when air content in argon atmosphere exceeded about 0.6% for electron-beam melted pure molybdenum and powder metallurgy TZM alloy. In less than 0.26% air, no hot cracking were observed in this experiment. Moreover, in electron-beam welding, no hot cracking was observed in weld metals for both materials. In order to prevent the formation of hot cracking, the purity of welding atmosphere should be kept as high as possible. (3) Joint efficiency of the welded joint of electron-beam melted pure molybdenum with electron-beam welding was 50 to 60% to base metal at room temperature and 500°C and almost 100% at 1000°C. Those of GTA welds in pure and 0.13% air mixed argon atmospheres were fairly lower than those in electron-beam welding for each testing temperature.

KEY WORDS: (Molybdenum) (Weldability) (Cracking) (Porosity) (Defects) (Electron Beam Welding) (GTA Welding)

1. Introduction

Molybdenum has many properties which would make it an useful structural material for many high temperature uses.

Recently, there is paid an attention to use molybdenum metal for the first wall material in some experimental fusion reactor vessels in Japan. For the fabrication of the first wall, fusion welding techniques of molybdenum metal are also strongly expected. However, the major drawback to the use of molybdenum structures is poor weldability in fusion welding as high susceptibility to cracking and porosity in weld metal due to impure welding atmosphere and low weld bend ductility near room temperature due to impurity and coarse grain in weld metal.

Many research programs have been conducted to overcome the poor weldability in the above during 1950' to 1960' years^{1~12)}. Some important gains were made with the discovery that fairly sound and ductile welds

could be made by GTA welding process in conventional molybdenum under high-purity dry-box atmosphere. However, those investigations have been mostly done for powder-metallurgy or arc-cast molybdenum whose purity is not so high.

During these ten years, both electron-beam melting and welding processes in high vacuum have been developed much. Therefore, high pure molybdenum metal can be easily obtained by electron-beam melting and high pure weld of molybdenum also performed by electron-beam welding.

This study was investigated to make clear the weldability of electron-beam melted high pure molybdenum metal using electron-beam welding in high vacuum and GTA welding in pure and impure argon atmospheres.

In the first report I, the effect of welding atmosphere on weld defects, such as cracking and porosity and mechanical properties were treated, and in the report II weld metal bend ductilities will be treated.

[†] Received on September 18, 1979

* Professor

** Associate Professor

*** Research Associate

**** Graduate student, KANSAI Univ.

Transactions of JWRI is published by Welding Research Institute of Osaka University, Suita, Osaka, Japan

2. Materials Used and Experimental Procedure

2.1 Materials used

The electron-beam melted pure molybdenum (EB-Mo) has been mainly used in this experiment. It is the most pure molybdenum obtained in commercial levels and contains a little carbon. In addition, as molybdenum alloys in comparison with EB-Mo, two sorts of TZM (Mo-Ti-Zr) alloys, which are one of the most common commercially used molybdenum alloys, have been also used. One of them is a vacuum arc-melted TZM (AM-TZM) and another is a powder-metallurgy one (PM-TZM).

Table 1 Chemical composition of materials used

Material	Chemical composition (ppm)								
	O	N	C	Si	Ni	Fe	Ti	Zr	Mo
EB-Mo(40C)	8	12	40	88	1	2	-	-	Bal.
AM-TZM	3	<1	170	<10	<10	10	4000	910	Bal.
PM-TZM	200	8	380	-	-	-	5000	700	Bal.

Chemical compositions of these materials are shown in Table 1. It is well known that oxygen and nitrogen are very harmful elements to the weldability of molybdenum materials^{6), 9)}.

Therefore, the contents of these elements in EB-Mo and AM-TZM are lowered to the minimum, that is, about 10 ppm or less, but oxygen content in PM-TZM is much more, that is, 200 ppm.

The sheet thickness of these materials is 1.5 mm and all materials used were annealed for the stress relieving.

2.2 Experimental procedure

2.2.1 Welding method

As welding method, electron-beam welding (EBW) in high vacuum (1×10^{-4} Torr) has been used in order to examine the weldability of molybdenum materials under the condition that the contamination from welding atmosphere was negligible.

In addition, on the contrary, in order to examine the effect of the purity of the welding shielding gas on the

weldability, inert gas tungsten-arc (GTA) welding has been performed in a welding chamber initially evacuated to 1×10^{-3} Torr and filled to 760 Torr with a high purity argon gas (99.99% Ar) or its mixing gas of air as a shielding gas of welding. The air in argon gas has been mixed up to about 1% in volume.

Two series of the welding conditions which produced the full penetration were selected in each welding method. They are listed in Table 2. In the case of GTA welding arc voltage was kept to a constant value of about 11 volt. Only full penetrated bead-on-plate welding was used in this work. The dimensions of weld specimens are 40 mm in width, 210 mm in length and 1.5 mm in thickness. Welding direction was perpendicular to the rolling one of the sheet. Weld specimen was clamped to a copper backing plate in order to suppress the distortion in each welding method.

Moreover, to insure a clean surface for welding, all specimens were etched in a solution containing 95 parts H_2SO_4 , 4.5 parts HNO_3 , 0.5 part HF and 18.8 g per liter Cr_2O_3 ⁷⁾.

Specimens were immersed in the solution for ten min, then rinsed in a running water and cleaned with acetone.

2.2.2 Radiographic and metallurgical examinations

Occurrence of weld defect such as cracking and porosity in weld metal has been investigated by the x-ray radiographic examination.

Moreover, the metallographic examination has been made mainly on the cross-sections of weldments by the optical microscope and scanning electron microscope (SEM) with X-ray microanalyzers of an energy dispersive type (EDX) and a wave dispersive type (WDX) in order to examine the relation between weld structure and weld defects, and also weld structural changes caused by the variations of welding conditions and purity of welding atmosphere. The specimens were polished electrolytically in a electrolyte of CH_3OH with 12.5% H_2SO_4 and etched by Murakami's etchant¹³⁾.

Moreover, the hardness measurement of welded joint has been carried out on cross-section.

Table 2 Welding conditions used

Welding method	Welding condition	
EBW	50 kV, 55 mA, 2540 mm/min	1×10^{-4} Torr
	50 kV, 45 mA, 1000 mm/min	
GTAW (dcsp)	11 V, 150 A, 100 mm/min	Ar (99.99%) or Ar + Air (Max. 1.05%) 1 atm.
	11 V, 170 A, 100 mm/min	

2.2.3 Hot tension test

Hot tension test has been performed for base metal and welded joints of EB-Mo for EB and GTA welding in pure argon and in air mixed argon atmosphere at room temperature (26°C), 500 and 1000°C. At elevated temperature, vacuum electric furnace evacuated to a degree of 1×10^{-4} Torr was used to protect tensile specimen from the oxidation. The size of specimen is shown in Fig. 1

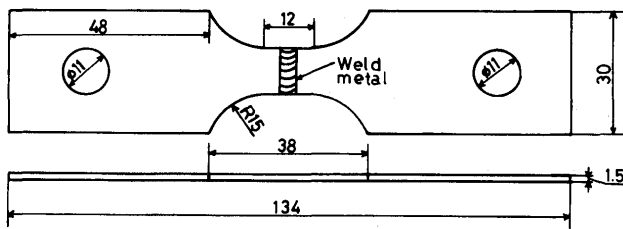


Fig. 1 Dimensions of hot tension test specimen

3. Results and Discussions

3.1 Gas absorption into weld metal from welding atmosphere

The relation between oxygen and nitrogen contents and partial pressure of air gas in argon welding atmosphere are shown in Fig. 2 for the GTA welds of EB-Mo and PM-TZM.

As to oxygen content, in the case of EB-Mo, oxygen content did not increase as an increase of air content up to 0.26%. However, over 0.56% air, it abruptly increased.

This is considered to be related closely to the formation of hot cracking due to molybdenum oxide as mentioned in section 3.3.

On the other hand, for PM-TZM, oxygen content increased almost linearly with increase of air content and it is always much more than that of EB-Mo in the same air partial pressure.

This is mainly due to its high oxygen content of base metal of PM-TZM, that is, 200 ppm. In weld metal in pure argon, however, it remarkably decreased to about a half of base metal, that is, 90 ppm. The reason above seems to be that molybdenum oxide containing in base metal because of powder-metallurgy method was decomposed or vaporized by melting by welding arc.

On the other hand, nitrogen content increased almost linearly for both materials with the increase in air content, though its amount of PM-TZM was much more than that of EB-Mo at the same air partial pressure. That is, the absorption of nitrogen into weld metal is about two times larger than that of EB-Mo. This seems to be caused by Ti or Zr which is main alloying element for TZM and has a good affinity for nitrogen.

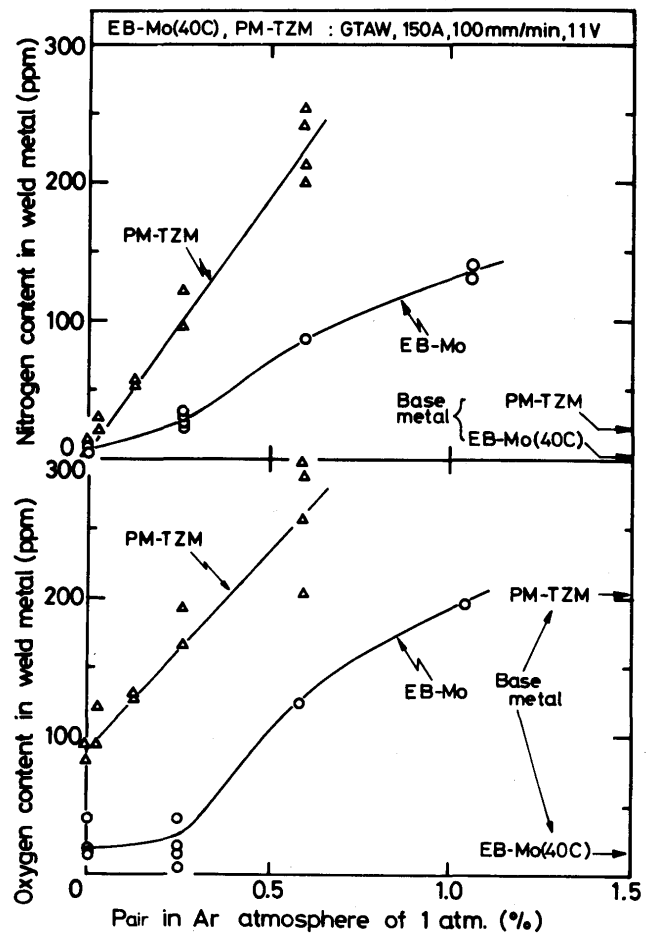


Fig. 2 Effect of air content in welding atmosphere on oxygen and nitrogen contents of weld metal of EB-Mo(40C) and PM-TZM

3.2 Weld porosity

The effect of the purity of welding atmosphere on the formation of porosity has been examined in the weld metals of EB and GTA weldings for two types of materials. One is EB-Mo or AM-TZM containing very little amounts of oxygen and nitrogen and another is PM-TZM which contains much more amounts of oxygen, that is, 200 ppm but very little amount of nitrogen. The results are shown in Fig. 3 whose vertical axis indicates the number of blowhole observed on the X-ray radiographic film of weld bead of 200 mm in length.

In the case of GTA welding, as shown in the right side in Fig. 3, the effect of air content mixed in argon welding atmosphere on the formation of porosity in weld metal has been examined for EB-Mo and PM-TZM. There were little blowholes observed in each material, even in less pure argon atmosphere mixed with air gas up to about 0.6% for PM-TZM and about 1% for EB-Mo.

On the other hand, as shown in the left side in Fig. 3, for EB welding in high vacuum, the formation of blow-

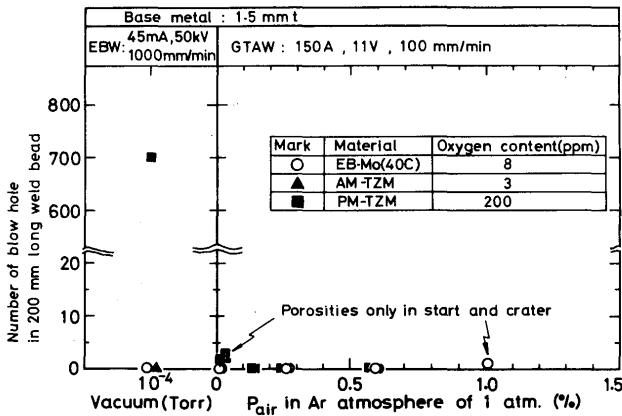


Fig. 3 Effect of air content mixed in welding atmosphere on occurrence of porosity in weld metal of electron-beam and GTA weldings (Materials; EB-Mo(40C), PM-TZM and AM-TZM)

hole has not been observed in the weld bead of EB-Mo and AM-TZM, which contain very little oxygen and nitrogen less than 10 ppm. In the case of PM-TZM, however, a lot of blowholes have been observed as shown in Fig. 4

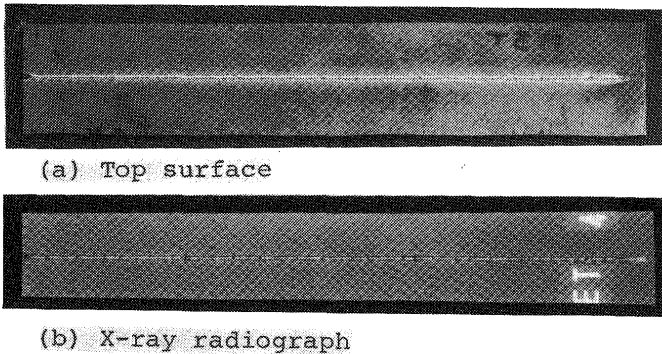
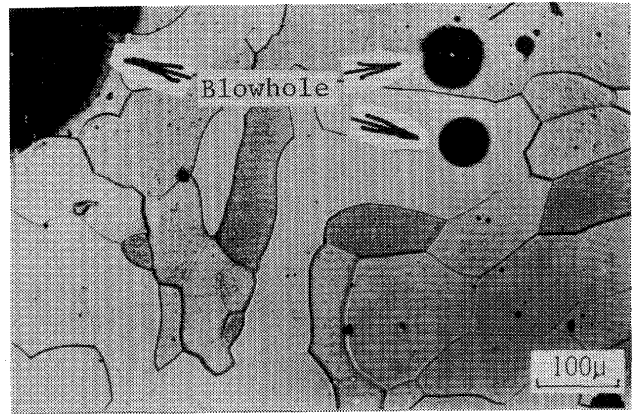


Fig. 4 Top surface of weld bead of PM-TZM and its X-ray radiograph (EBW; 45 mA, 50 kV, 1000 mm/min)

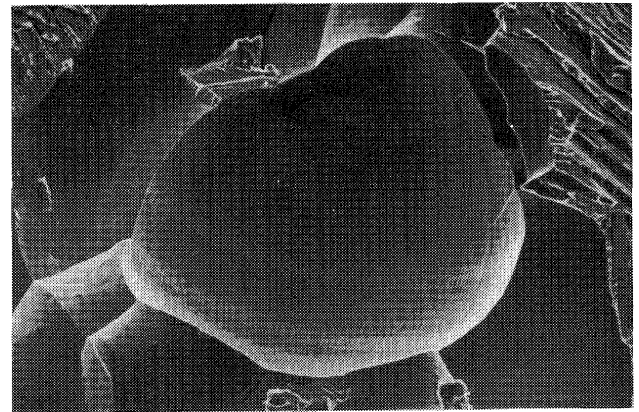
which show a very porous weld bead. Figure 5(a) and (b) also show its microphotograph and inner surface of blowhole observed by SEM showing dendritic pattern, respectively. These weld porosities are considered to be caused by its high oxygen content of the base metal of PM-TZM.

On the contrary, as mentioned above, blowhole has been little observed in GTA welding even for PM-TZM. As the reason above, the very rapid cooling rate at the solidification during EB welding is considered to one of the reasons besides its high vacuum of welding atmosphere. Because of this rapid cooling rate, the blowholes formed in molten pool seemed to be confined in solidified weld metal not to be able to escape out of molten weld pool.

As a result, in order to prevent the formation of weld porosity, it is needed to base metal that oxygen content in it should be lowered to the minimum as less than 10 ppm



(a) Microphotograph



(b) Inner surface

Fig. 5 Microphotographs of blowholes and its inner surface observed by SEM (Material; PM-TZM)

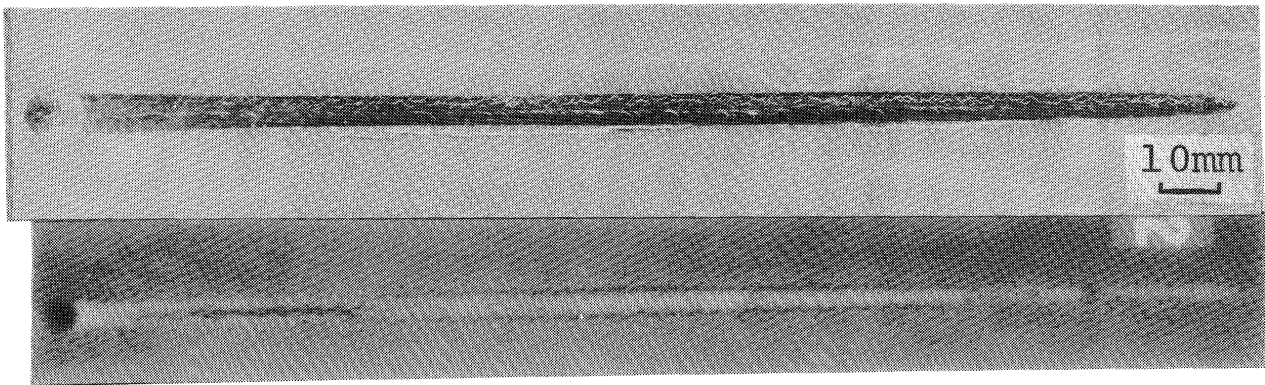
especially in EB welding in high vacuum. It seems that the same attention should be also paid to nitrogen content of base metal.

3.3 Weld hot cracking

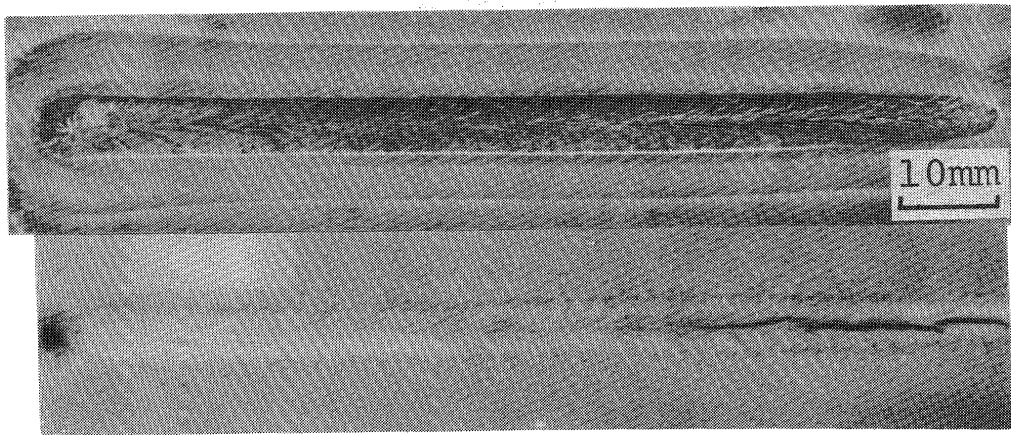
The weld hot cracking is the most serious defects in fusion welding of molybdenum. It was reported that oxygen and nitrogen in welding atmosphere caused hot cracking in the weld bead of molybdenum, especially oxygen was the most harmful⁶⁾. In actual GTA welding process for the industrial purpose, it is generally performed under an open air condition.

In this condition, welds is considered to be always contaminated to some degrees by air gas involved into welding atmosphere from surrounding air. Therefore, it is very important to examine the effect of air content in welding atmosphere on the formation of hot cracking.

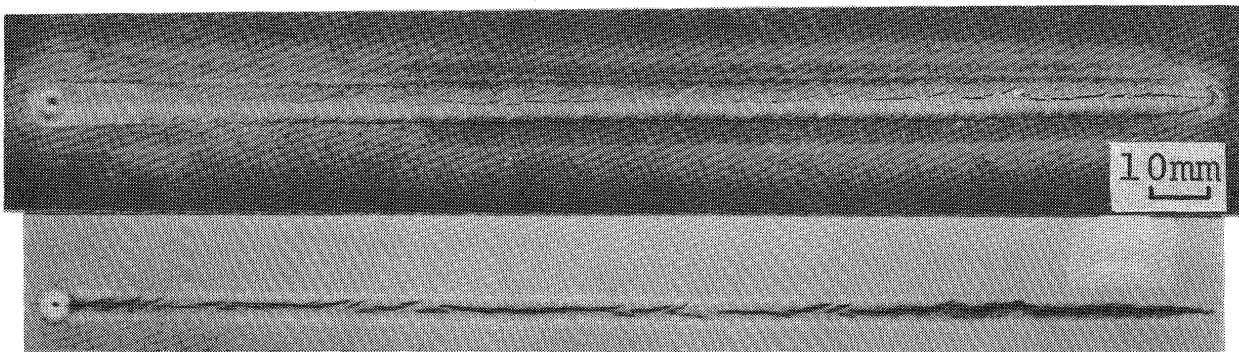
In the case of GTA welding with air mixed argon atmosphere, increasing air content, cracking has become appeared in the center of weld bead as shown in Fig. 6(b) and (c) in comparison with (a) with pure argon atm-



(a) Pure Ar



(b) Ar + 0.59% air



(c) Ar + 1.05% air

Fig. 6 Top surface of weld beads of EB-Mo and their X-ray radiographs for various air contents in welding atmosphere (GTAW; 150 A, 11 V, 100 mm/min)

osphere for EB-Mo. According to the observation through eyes during welding, these cracks were initiated just behind welding puddle during welding. Therefore, they seem to be hot cracking. These center-bead cracks were measured their lengths on the X-ray radiographic film.

The relation between crack length and air content in argon atmosphere is shown in Fig. 7 in which the result of EB welding is contained. As to the EB-Mo welds, the

cracks have not been observed in weld bead in the case of high purity and air mixed argon atmosphere up to 0.26%. Increasing air content to 0.59%, however, the center-bead crack began to be observed as shown in Fig. 6(b) but its length was still short. At 1.05% air the entire weld bead was cracked as shown in Fig. 6(c). The quite similar effect of air gas has been observed in the weld bead of PM-TZM.

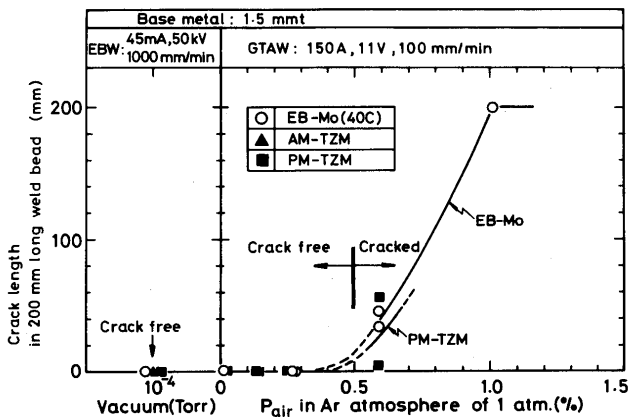


Fig. 7 Effect of air content mixed in welding atmosphere on occurrence of hot cracking in weld metal of EBW and GTAW (Materials; EB-Mo(40C), PM-TZM and AM-TZM)

Therefore, the threshold value of air content in argon atmosphere is considered to be in the range of 0.26 to 0.59% for EB-Mo and PM-TZM in this experiment, though this value may shift according to a degree of the restraint of weld specimen.

On the other hand, in the case of EB welding, where the contamination from welding atmosphere is considered to be negligible, no cracks have been observed in the weld beads of EB-Mo, AM-TZM and PM-TZM.

As a result, in order to prevent the formation of hot cracking in weld bead, the contamination of air gas into welding argon atmosphere should be made to be minimum.

Figure 8 shows the cracked surface of the center-bead crack formed in the weld bead of EB-Mo. The center-bead crack is intergranular one and its surface appears to be smooth as shown in Fig. 8(a), but it is covered with substances making networks. SEM microphotographs in

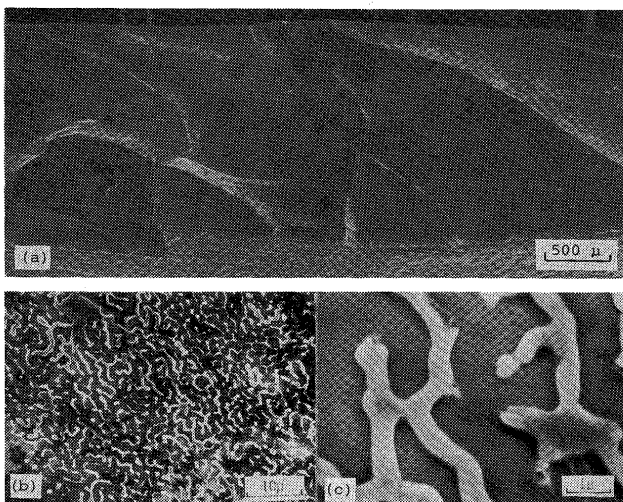


Fig. 8 SEM microphotographs of inclusions on hot cracked surface

high magnification makes clear the details of these network formers as shown in Fig. 8(b) and (c). These networks have not been observed except the hot cracking surfaces. Therefore, it seems that they are one of the causes of hot cracking. Figure 9 shows the results of

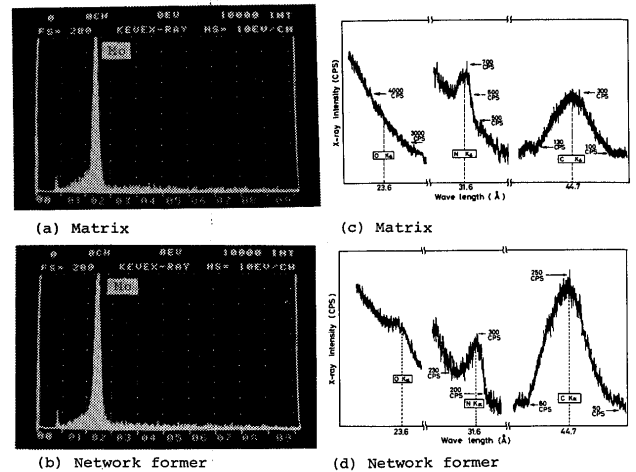


Fig. 9 Results of X-ray analysis by WDX and EDX for hot cracked surface (Material; EB-Mo(40C))

X-ray analysis by EDX and WDX about the matrix and the network former on the cracked surface. According to the result of EDX, molybdenum only has been detected in each case as shown in Fig. 9(a) and (b). On the other hand, in the WDX result as shown in Fig. 9(c) and (d), carbon and nitrogen were detected in each case at the peaks at 44.7 and 31.6 Å of the wave length, respectively, but oxygen peak at 23.6 Å was detected only in the network former, though there is no peak in matrix.

As the results of EDX and WDX, these networks are considered to be molybdenum oxide. Therefore, it is considered that the low melting point eutectic of molybdenum oxide-molybdenum causes the hot cracking when the deformation or the strain due to welding is applied to the grain boundaries liquated.

3.4 Structure and hardness in welds

3.4.1 EB and GTA welds in pure argon atmosphere

Figure 10 shows the typical examples of the macrostructure in cross-section of the welded joints for EB and GTA welding in pure argon atmosphere. As shown in Fig. 10(a), for an example, macrostructure of welded joint consists of base metal showing fibrous structure, heat affected zone (HAZ) showing recrystallized structure and weld metal of columnar crystals.

Comparing the macrostructure of EB welds with that of GTA welds for EB-Mo, as shown in Fig. 10(a) and (d),

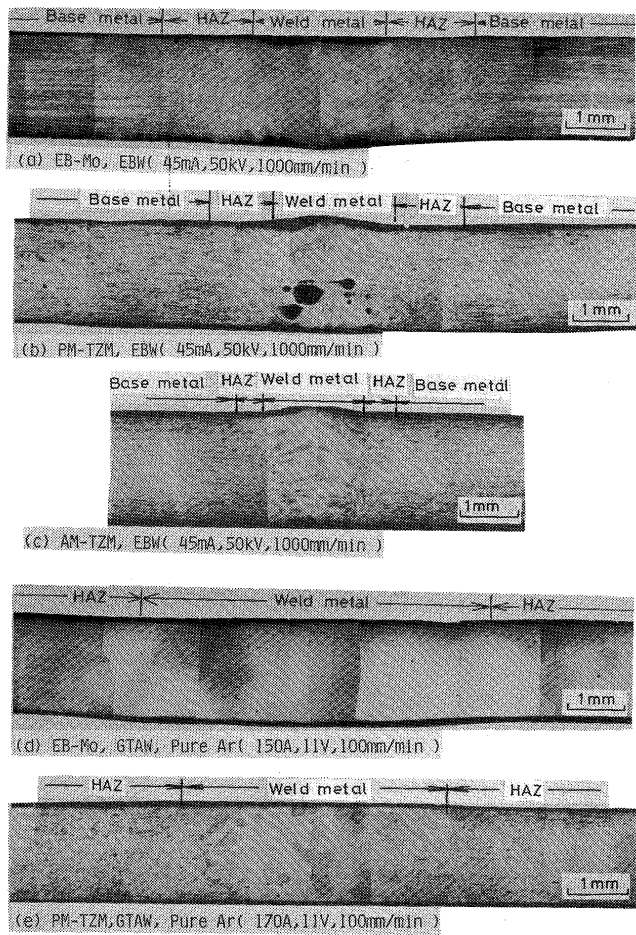


Fig. 10 Macrostructures on cross-section of welds of EB-Mo, PM-TZM and AM-TZM for various welding heat input

respectively, the width of fusion zone and HAZ for EB welds were much narrower than those of GTA welds. Moreover, the grain size in each region, which become much larger than those of base metal, is much smaller in EB welds than those in GTA welds. This is the cause that weld heat input in EB welding is much less than that in GTA welding under the same depth of weld penetration. For an example, in the case of Figure 10(a) and (d), weld head input in EB welding is only about one seventh of that in GTA welding. These differences in macrostructures between EB and GTW welds have been also observed similarly for TZM alloys. Therefore, in order to suppress the coarsening of grains in the fusion zone and HAZ to the minimum, EB welding is more excellent welding method than GTA welding.

On the other hand, comparing EB-Mo with TZM alloys, there were obvious differences in macrostructures of weld metal and HAZ. That is, the grain sizes in each region of TZM alloys were fairly smaller than those of EB-Mo in each welding method. It is considered that this is mainly due to higher recrystallization temperature of TZM alloys, that is, about 1400 - 1600°C¹⁴⁾ than that of EB-Mo,

about 1000 - 11000°C¹⁵⁾. In addition, the widths of fusion zone and HAZ of TZM alloys is fairly narrower than those of EB-Mo, which are more obviously shown in Fig. 10(e) in comparison with (d). It seems that the diameter of electron-beam during welding was concentrated to be finer by the vapor having relative high partial pressure of Ti and Zr alloying elements in TZM in the case of electron-beam welding.

Nextly, hardness distribution of welded joint which is considered to be one of the significant factors affecting the mechanical properties has been investigated on the cross-section of welded joint. The typical examples of the distributions of hardness of welded joint are shown in Fig. 11 for EB and GTA welds of EB-Mo. In both welding

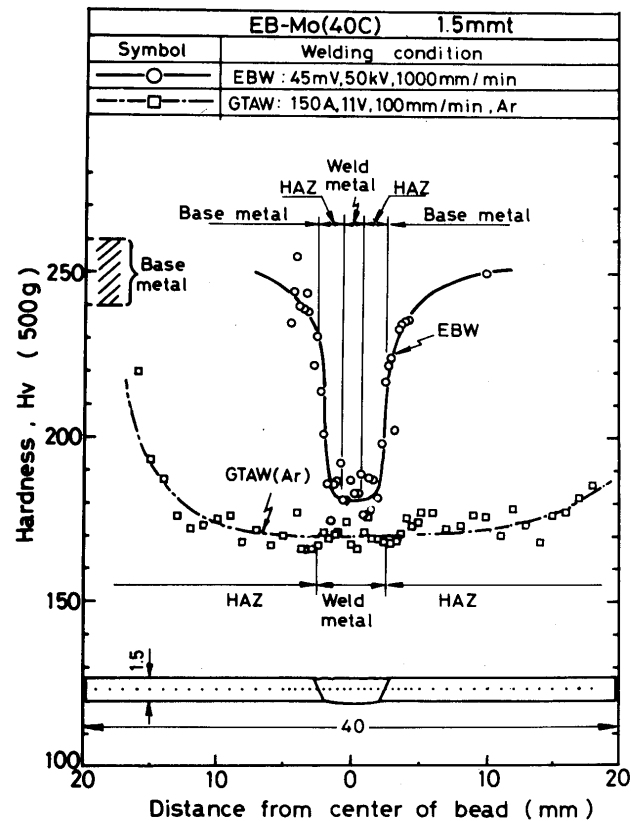


Fig. 11 Typical examples of distribution of hardness in EBW and GTAW welds for EB-Mo(40C)

methods, the hardnesses of weld metal and HAZ became very low in comparison with that of base metal.

In addition, for EB welding, they were slightly higher than for GTA welding. Moreover, the softened range in EB welding is much narrower than that in GTA welds because of its lower welding heat input as described previously.

There were a remarkable difference in hardness of the welded joints between EB-Mo and PM-TZM under the same welding condition, which are shown in Fig. 12 for

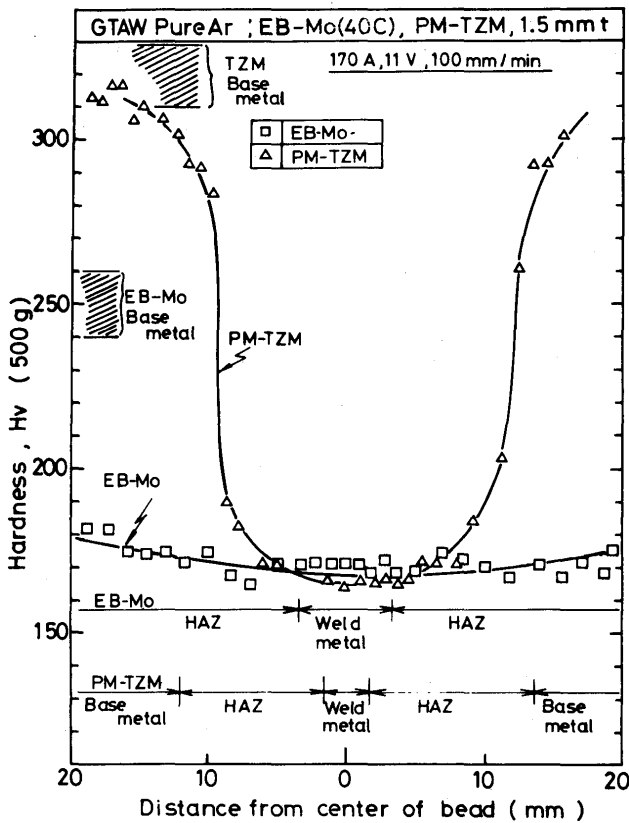


Fig. 12 Difference in hardness of GTA welds of EB-Mo(40C) and PM-TZM under same welding condition

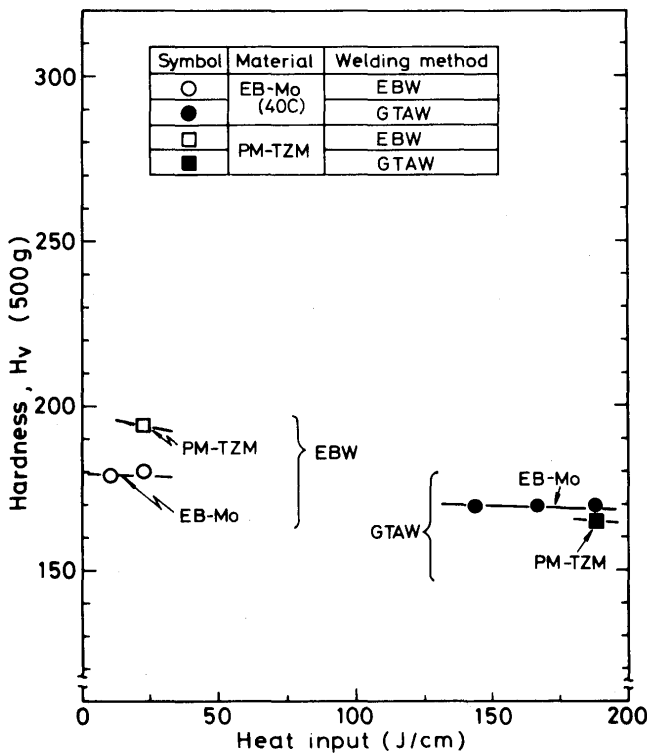
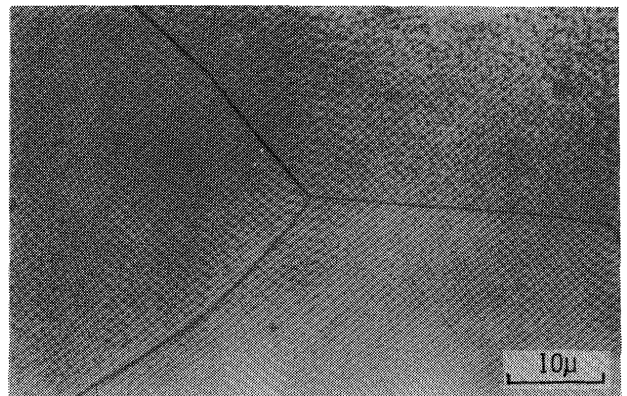


Fig. 13 Relation between hardness of weld metal of EB-Mo(40C) and PM-TZM and welding heat input, EI/V(J/cm)

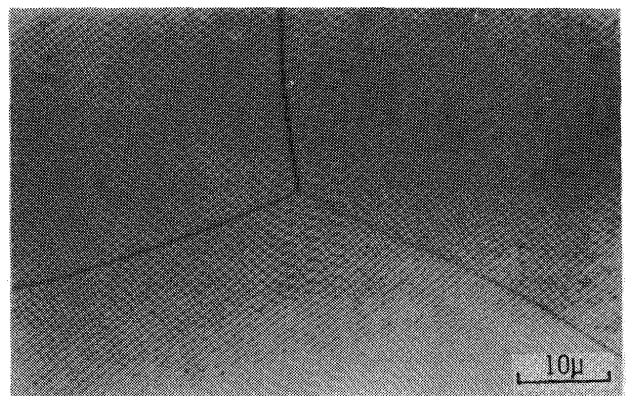
GTA welds. Weld metal and HAZ were significantly softened similarly for each materials. However, this softened range for PM-TZM was much narrower than that of EB-Mo because of higher recrystallization temperature of PM-TZM.

The maximum hardnesses measured in weld metal are shown in Fig. 13 against welding heat input(joule/cm). As a result, the hardness tends to decrease as the increase of welding heat input for EB-Mo and PM-TZM, though for EB-Mo, there were no remarkable differences in hardness against the small variation of heat input in each welding method, respectively. However, in case of large variation of heat input, such as, in comparison with EB and GTA welds, they became slightly higher in EB than those in GTA welds.

Microstructures of the weld metals are shown in Fig. 14(a) and (b) for EB-Mo and PM-TZM, respectively, in the same welding condition of EB welding. There were no obvious precipitates in both materials.



(a) EB-Mo(40C)



(b) PM-TZM

Fig. 14 Typical examples for microstructures of weld metals of EB-Mo(40C) and PM-TZM

3.4.2 GTA welding in air mixed argon atmosphere

The effect of air gas in argon atmosphere of GTA welding on weld structure and hardness has been examined for EB-Mo and PM-TZM.

The weld bead appearances of EB-Mo are shown in Fig. 15 against various contents of air gas in argon atm-

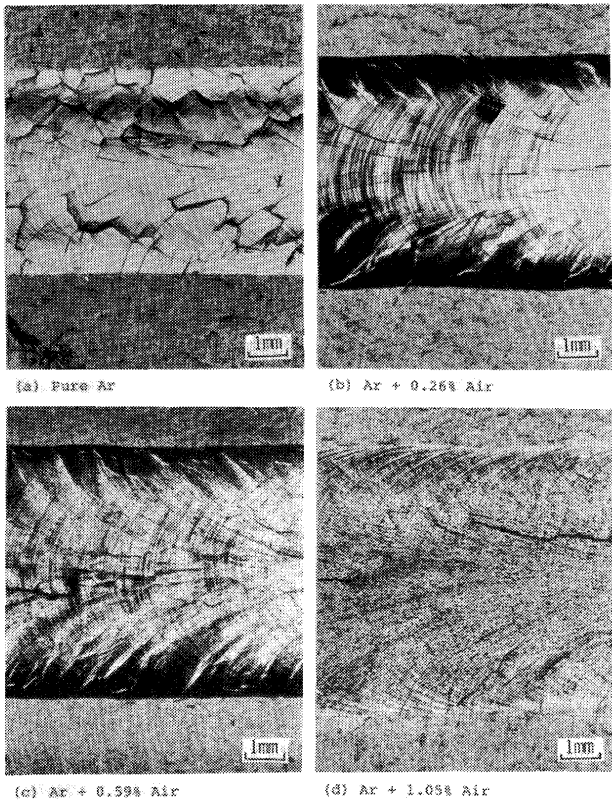


Fig. 15 Influence of air content mixed in welding atmosphere in GTAW on appearance of weld bead surface for EB-Mo(40C)

osphere. The weld bead surface was very clean up to 0.26% air. Increasing air content more than 0.59%, however, it became dark colored appearance due to the oxidation by air.

Increase in air gas in welding atmosphere also caused the increase in the width of fusion zone, which was considered to be due to the increase in arc voltage.

Hardness distribution has been measured on the cross-section of the welded joint. Typical examples are shown in Figs. 16 and 17 for EB-Mo and PM-TZM, respectively, with and without air gas in welding atmosphere. The air gas tends to increase the hardness of the weld metal in both materials. The increase in hardness is much larger in PM-TZM than EB-Mo.

This is also obviously shown in Fig. 18 which shows the effect of air content on the maximum hardness of weld metal. In the case of EB-Mo, the increase in the

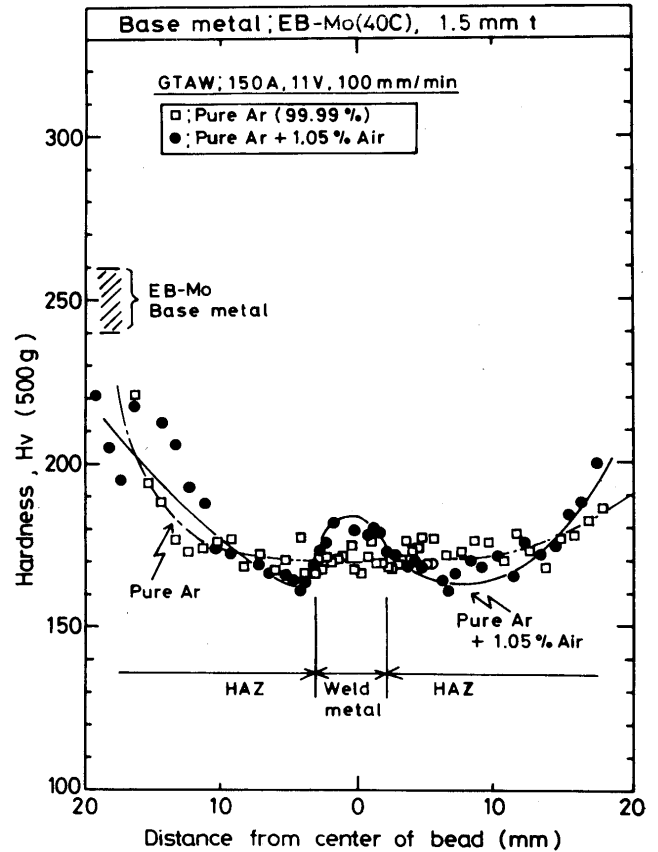


Fig. 16 Difference in distribution of hardness in GTA welds of EB-Mo(40C) caused by difference of air content in welding atmosphere

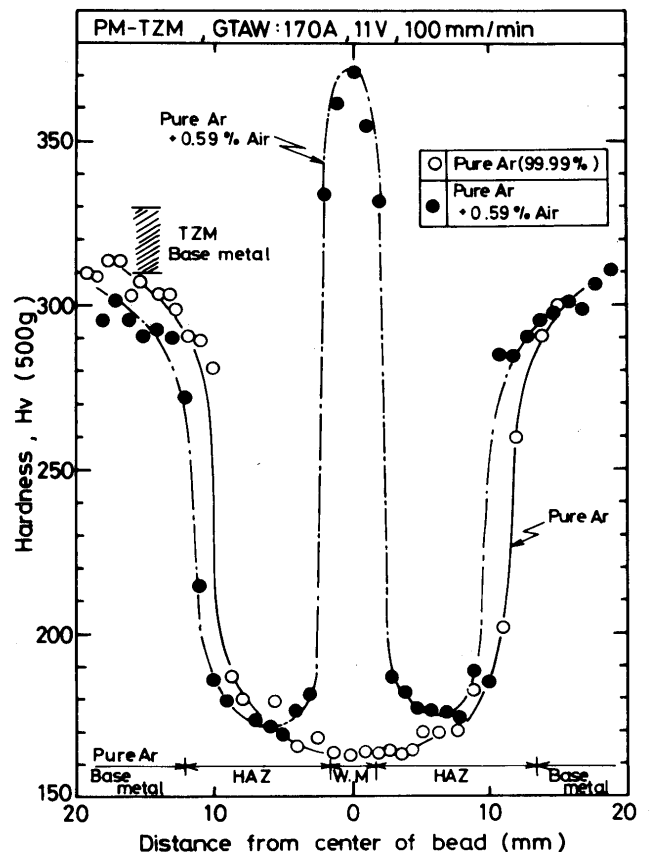


Fig. 17 Difference in distribution of hardness in GTA welds of PM-TZM caused by difference of air content in welding atmosphere

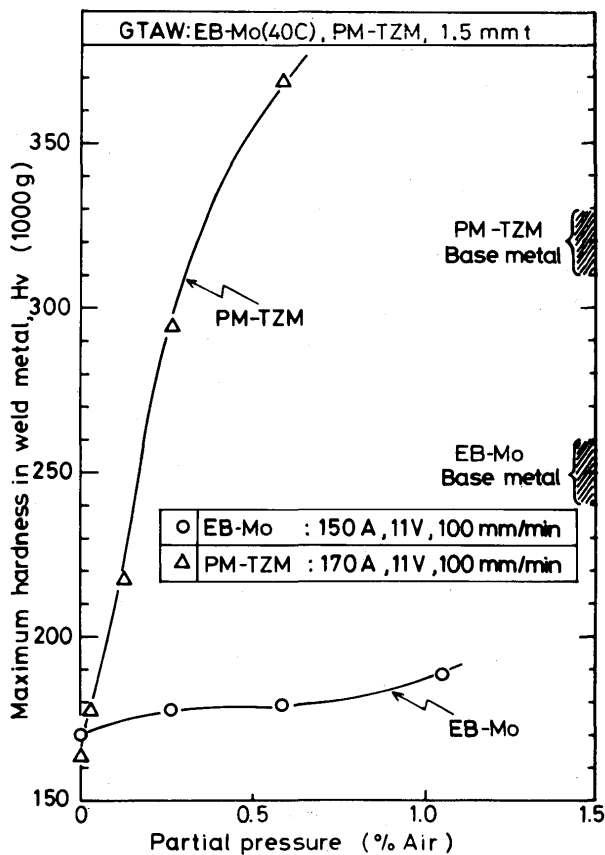


Fig. 18 Effect of air content in welding atmosphere on maximum hardness of weld metals of EB-Mo(40C) and PM-TZM

hardness for air content is very small, that is, about 190(Hv) at 1.05% air against 170(Hv) at pure argon. On the contrary, as to PM-TZM, hardness has remarkably increased as increase in air content. Especially, only at 0.59% air, it was increased to 370(Hv). This is two times of that at pure argon, and also more than that of base metal. Hence, the hardnability of the weld metal of PM-TZM at air mixed atmosphere is quite large. It seems that this is due to results of the reaction of its alloying element of Ti or Zr with nitrogen or oxygen.

Nextly, effect of air gas in welding atmosphere on weld microstructure has been examined. Figures 19 and 20 show the microphotographs for EB-Mo and PM-TZM, respectively. As to EB-Mo, precipitates increased its amount as the increase in air content. That is, in the case of pure argon, there were no obvious precipitates in the matrix and grain boundary, though the zigzag shaped grain boundaries observed sometimes suggests the existence of the very fine precipitates in grain boundaries, which seems to be molybdenum carbides. As the increase in air content more than 0.26%, the precipitates became obviously observed in grain boundaries. Moreover, the precipitates almost continuously occupied grain boundaries at 1.05% air. On the other hand, in the matrix, the needle

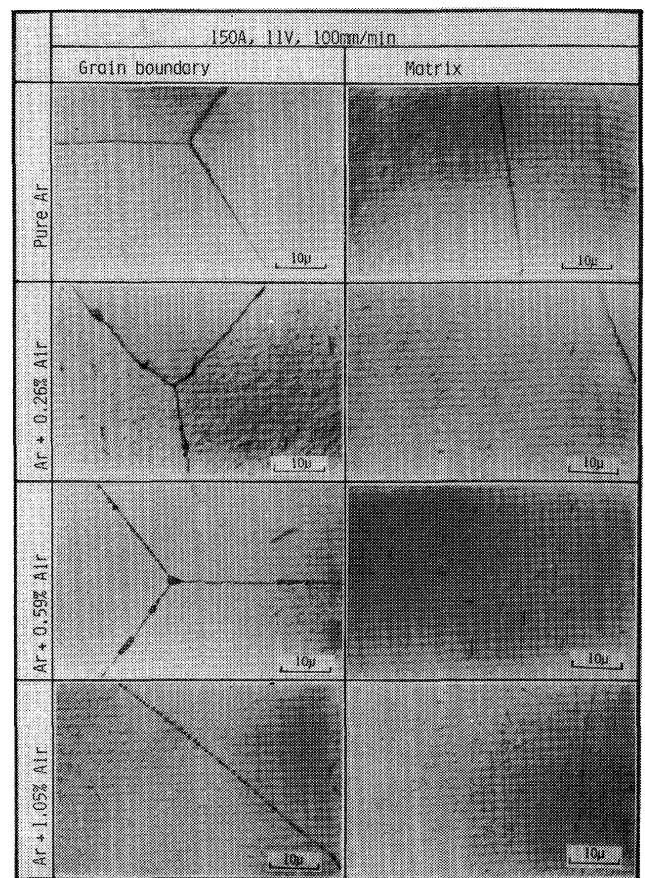


Fig. 19 Microphotographs of weld metals of EB-Mo(40C) with GTAW for various air contents in welding atmosphere

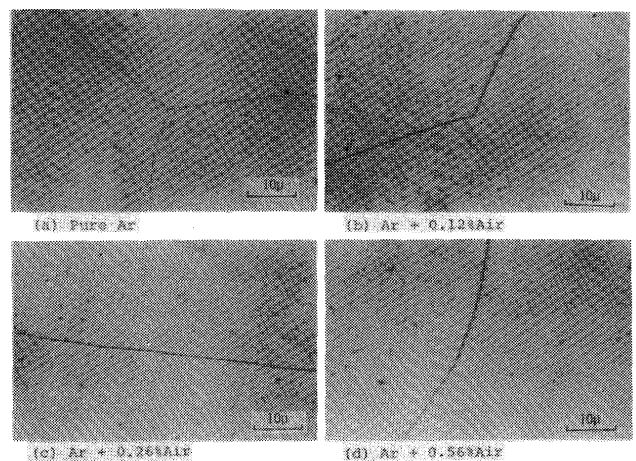


Fig. 20 Microphotographs of weld metals of PM-TZM with GTAW for various air content in welding atmosphere

like precipitates became observed at 0.26% air and its amount was increased as the increase in air content. These needle like precipitates seem to be molybdenum nitride⁹⁾.

On the contrary, in the case of PM-TZM, the zigzag shaped grain boundaries have been observed much more

than in the case of EB-Mo even in pure argon. As the increase in air content, however, these were no obvious precipitates in grain boundaries such as those observed in EB-Mo though spherical precipitates observed mainly in matrices increased its amount, which is said Titanium oxide⁶). Moreover, the fine needle like precipitates such as observed in EB-Mo began to be observed in the matrices at air content more than 0.26%, though their amounts seemed to be less than those in EB-Mo.

The fractographic investigations of the precipitates will be discussed in the report II.

3.5 Mechanical properties of welded joint at high temperature

The specimens after hot tension tested are shown in Fig. 21 for EB-Mo. All test pieces were free from weld defects such as hot cracking and porosity.

Figure 22 indicates tensile strength and elongation against testing temperature for each specimen. The tensile strength of base metal of EB-Mo is about 80 Kg/mm² at room temperature. As the increase in the testing temperature, it was linearly decreased to about 20 Kg/mm² at 1000°C. As to welded joint, the tensile strength was also decreased in testing temperature. In the case of EB welds, at room temperature and 500°C, the tensile strength was about one half lower than those of base metal, but at 1000°C, it became almost the same as that of base metal.

On the contrary, for GTA welds with pure and air mixed argon atmospheres, the tensile strength was not able to be measured at room temperature because of fracture during setting of specimen in testing machine.

This suggests that the welded joint of GTA welding has a poor ductility near room temperature. The tensile strength of GTA welds was a little lower than that of EB welds at 500 and 1000°C.

Nextly, the elongations of base metal and EB welds increased as the increase in testing temperature. At room temperature, the elongation of EB welds was fairly low, that is, about 4% in comparison with that of base metal, that is, 15-20%. On the contrary, at 500°C for GTA welds, they were much larger, that is, about 30-35% than those of base metal and EB welds. This is understood by the reason that the softened range in welds such as weld metal and HAZ as previously described in section 3.4 is much wider in GTA than in EB welds and moreover, the plastic deformation tends to concentrate mainly in this softened range. Then, at 1000°C, it slightly decreased to almost same value of about 20 to 30% as those of base metal and EB welds. The air gas of 0.13% in welding atmosphere slightly lowered the elongations and elevated the strength at elevated temperature due to contamination.

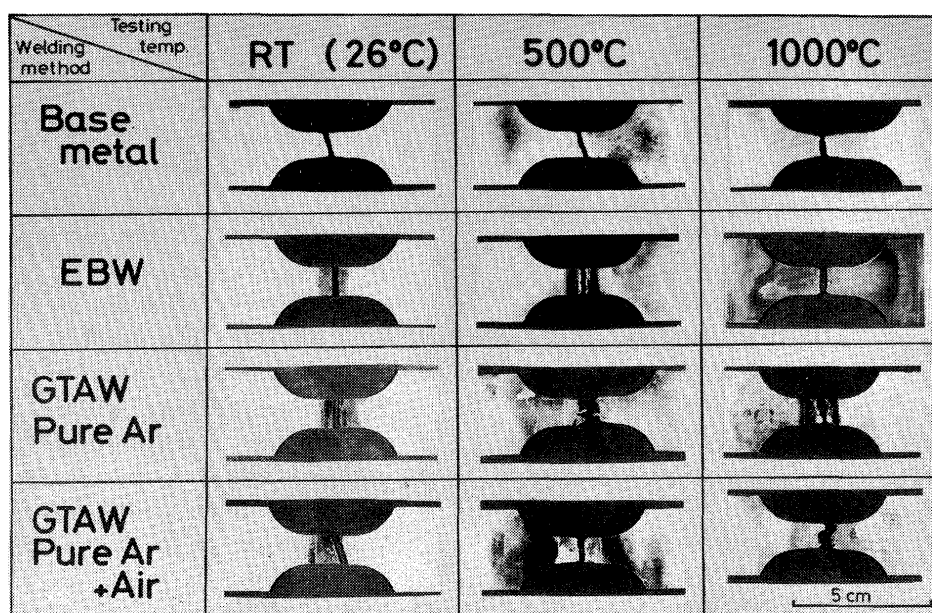


Fig. 21 General appearance of hot tension-tested specimen of EB and GTA welds of EB-Mo(40C)

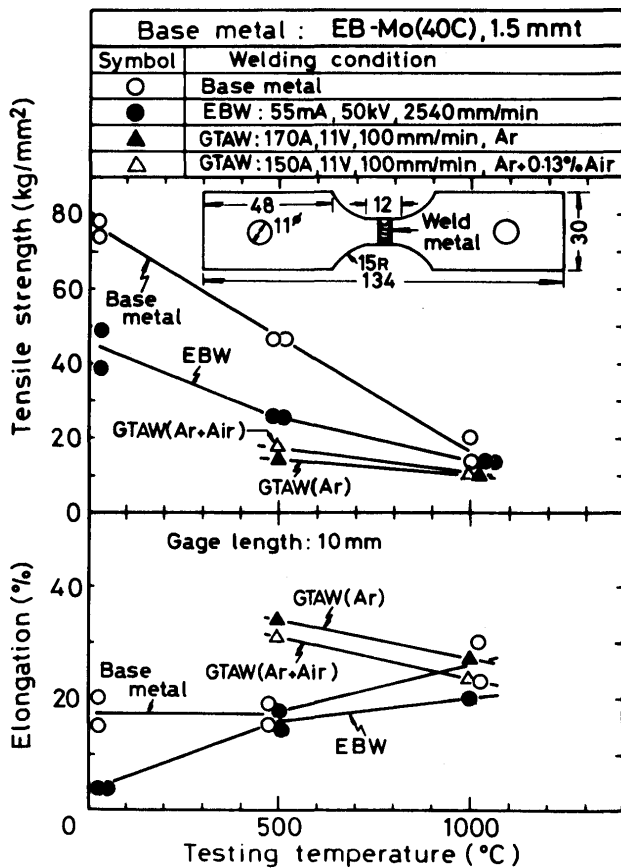


Fig. 22 Tensile strength and elongation of EB and GTA welds for various testing temperatures

4. Conclusions

The basic weldability of electron-beam melted high pure molybdenum has been examined with electron-beam welding in high vacuum and GTA welding in pure and air mixed argon atmospheres by paying the attention to weld defects such as hot cracking and porosity in weld metal and also mechanical properties of welded joint in comparison with conventional TZM alloys.

The main conclusions obtained are as follows;

- (1) Oxygen and nitrogen contents in weld metal were increased as the increase in air content in argon atmosphere of GTA welding. Those of electron-beam melted pure molybdenum were fairly less than those of powder-metallurgy TZM alloy for same air content.
- (2) Regarding to weld porosity, in the case of electron-beam melted pure molybdenum, porosity free weld was obtainable in the weld metal of electron-beam welding. In the case of GTA welding in pure argon and air mixed argon atmosphere up to about 1%, a few blowholes were sometimes observed both at weld crater and arc start. On the other hand, as to TZM

alloy of powder-metallurgy, the similar tendency was observed in GTA welding in pure argon and air mixed atmosphere. However, in electron-beam welding, very much blowholes were observed in weld metal because of its high oxygen content of 200 ppm, but no blowholes were observed for arc-melted TZM containing low level of oxygen of 3 ppm even in the weld metal of electron-beam welding. Therefore, in order to prevent weld porosity, oxygen content of base metal should be lowered to the minimum, that is, less than about 10 ppm, especially in the case of electron-beam welding process in high vacuum. Similar attention should be also paid to nitrogen content of base metal.

- (3) As to weld hot cracking, so far as concerning electron-beam melted pure molybdenum, hot cracking did not occurred in electron-beam welding. In GTA welding in pure argon and air mixed argon atmospheres up to 0.26%, hot cracking did not also occurred, but increasing air content more than 0.56%, center-bead hot cracking occurred. Quite similar tendencies were observed in the case of TZM alloys. Therefore, for preventing the hot cracking, the purity of welding atmosphere should be kept as high as possible and maximum permissible limits to air content mixed in argon atmosphere is about 0.26% in this experiment.
- (4) Macrostructures of HAZ and weld metal were much coarsened especially in weld metal in comparison with that of base metal. these tendencies were more remarkable in GTA welding than in electron-beam welding whose welding heat input was generally much less than that in former. Moreover, the coarsening tendency in weld metal was remarkable in electron-beam melted pure molybdenum in comparison with TZM.
- (5) The hardnesses of weld metal and HAZ in electron-beam welding and GTA welding in pure argon atmosphere were remarkably decreased in comparison with that of base metal for both electron-beam melted pure molybdenum and TZM alloys in this experiment. Moreover, they tended to decrease slightly as the increase in welding heat input.
- (6) Air gas mixed in the argon atmosphere of GTA welding increased the hardness of weld metals. This is more remarkably observed in TZM alloy weld metal than electron-beam melted one.
- (7) The joint efficiency of the welded joint of electron-beam melted pure molybdenum in electron-beam welding was about 50 to 60% to base metal at room temperature and 500°C and almost 100% at 1000°C. Those of GTA welds in pure argon and 0.13% air

mixed argon atmospheres were 30 to 40 and 55% at 500 and 1000°C, respectively.

Acknowledgement

The authors wish to thank Mr.Y. MIYAKE, undergraduate student of KINKI Univ., for his valuable contributions to this work and would like to thank Dr.T. HASHIMOTO, professor of SHIBAURA Technical college, for his useful discussions for this work and Dr.H. IRIE and Mr.S. TSUKAMOTO, researchers of the National Research Institute for Metals for their devotional assistances to perform electron-beam and GTA welding. Gratefulness is also given to Mr.K. HIRAYAMA, research associate of OSAKA Univ., for his radiographic technique and Mr.T. SHIDA, senior welding engineer and Mr.K. FUNAMOTO, welding engineer in HITACHI Research Laboratory, HITACHI, LTD., for their devotional assistances to hot tension test.

References

- 1) IISI GOODMAN; W.J., Vol. 29 (1950), No.1, pp.37-44.
- 2) T. PERRY, H.S. SPACIL AND J. WULF; W.J., Vol. 33 (1954), No.9, pp.442-s - 448-s.
- 3) J.H. JOHNSTON, H.VDIN AND J.WULF; W.J., Vol.-33 (1954), No.9, pp.449-s - 458-s.
- 4) E.F. NIPPES AND W.H. CHANG; W.J., Vol. 34 (1955), No.3, pp.132-s - 140-s.
- 5) E.F. NIPPES AND W.H. CHANG; W.J., Vol. 34 (1955), No.5, pp.251-s - 264-s.
- 6) W.N. PLATTE; W.J., Vol. 35 (1956), No.8, pp.369-s - 381-s.
- 7) R.E. MONROE, N.E. WEARE AND D.C. MARTIN; W.J., Vol. 35 (1956), No.10, pp.488-s - 498-s.
- 8) N.E. WEARE, R.E. MONROE AND D.C. MARTIN; W.J., Vol. 36 (1957), No.6, pp.291-s - 300-s.
- 9) W.N. PLATTE; W.J., Vol. 36 (1957), No.6, pp.301-s - 306-s.
- 10) N.E. WEARE, R.E. MONROE AND D.C. MARTIN; W.J., Vol. 37 (1958), No.3, pp.117-s - 124-s.
- 11) K.M. KULJI AND W.N. KEARNS; W.J., Vol. 37 (1958), No.10, pp.440-s - 444-s.
- 12) R.E. DAVLAK, M. CHRISTENSEN AND A.L. LOWE, JR.; W.J., Vol. 40 (1961), No.5, pp.197-s - 201-s.
- 13) Metals Handbook, 8th edition, Vol. 8 (1973), pp.108-109.
- 14) A. SEMENIOK AND G.R. BRADY; W.J., Vol. 53 (1974), No.10, pp.454-s - 459-s.
- 15) T. Fujiwara, K. Katoh and Y. Ohtakara; J. of JIM, Vol.-41 (1977), No.3, pp.256-263(in Japanese).